https://www.scirp.org/journal/ns Natural Science, 2022, Vol. 14, (No. 9), pp: 364-385

Experimental Induction of Heterotrophic to Autotrophic Conversion, Realized by the Enforced Primary Endosymbiosis of Photosynthetic Bacteria onto Eukaryotic Amoebae

Yasuo Maeda[1], Tomoaki Abe[2]

[1]Department of Developmental Biology and Neurosciences, Graduate School of Life Sciences, Tohoku University, Aoba, Japan; [2]Institute of Biological Sciences, Faculty of Science and Engineering, Ishinomaki Senshu University, Ishinomaki, Japan

Correspondence to: Yasuo Maeda, kjygy352@ybb.ne.jp
Keywords: Evolution, Multinucleate Plasmodium, *Dictyostelium*, *Rhodobacter*, *Synechocystis*
Received: August 11, 2022 **Accepted:** September 26, 2022 **Published:** September 29, 2022

ABSTRACT

The primary endosymbiosis of cyanobacteria with primitive eukaryotes is assumed to have occurred in ancient times, leading to the formation of plants with chloroplasts. However, since this possibility has remained experimentally unproven, we tried to convert heterotrophic eukaryotes like protozoa to autotrophs with chloroplasts. For this, when eukaryotic and heterotrophic *Dictyostelium* cells were forcibly cultivated with two kinds of photosynthetic bacteria (the purple non-sulfur bacterium *Rhodobacter* and then the cyanobacterium *Synechocystis*) as food sources, unique autotrophic organisms consisting of multinucleate plasmodia and their derived amoeboid cells, which had very strange morphology and behaviors, were formed by endosymbiosis of the bacteria. In this case, long-term pre-cultivation with *Rdodobacter* seemed to be prerequisites for the formation of the autotrophic organisms. The resulting, green-colored plasmodium contained a number of *Synechocystis*-derived bodies in the cytoplasm. The measurement of chlorophyll fluorescence indicates that the *Synechocystis*-derived bodies are like chloroplasts giving the ability of photosynthesis. Only, since the fine structural characteristics and genetic background of the autotrophic multinucleate plasmodia and their derived-amoeboid cells are extremely strange, we discuss the possibility of thinking about those reasons.

1. INTRODUCTION

The primary symbiosis of cyanobacteria with primitive eukaryotes is assumed to have occurred one

billion or more years ago, leading to the formation of chloroplasts. However, this possibility has remained experimentally unproven. Autotrophy is a form of nutrition involving the synthesis of organic substances via CO_2 fixation, using reducing power obtained from inorganic substances that are found in plants, algae, and certain anaerobic bacteria. This is in complete contrast to the process of heterotrophy, which is a mode of respiration by which biopolymers are synthesized by consuming and decomposing organic matter to use as a carbon source as part of the food chain [1-3]. On the ancient earth, primitive heterotrophic eukaryotes containing mitochondria probably took in photosynthetic bacteria, such as cyanobacteria, as food via phagocytosis, and some of the captured bacteria were retained in the host cells without being digested in the cytoplasm. These chance events eventually resulted in a primary endosymbiosis and the development of photosynthetic organelles, such as chloroplasts that are present in plant cells. Although chloroplasts have long thought to have originated by endosymbiosis of a cyanobacterium, their subsequent evolutionary history has been considered to be somewhat complicated [4]. Intracellular symbioses between eukaryotic cells are known to occur in *Paramecium bursaria* and *Hydra viridis* etc., in which green unicellular algae, such as Chlorella, are coordinated by the secondary endosymbiosis [2, 5]. Ohkawa *et al.* (2011) [6] tried to reproduce experimentally the conditions mimicking the first contact and development of symbiosis between unicellular ciliate, such as *Paramecium bursaria*, and photosynthetic bacteria, such as *Synechocystis* spp. PCC 6803, as a model for studying the very early evolutional processes for the emergence of photosynthetic eukaryotes. They succeeded in producing chimeric *Paramecium* with *Synechocystis* taken in by phagocytosis [6]. However, it remains to be elucidated whether the chimeric organism obtained can grow and proliferate in an autotrophic manner.

The cellular slime mold *Dictyostelium i*s a social amoeba widely distributed in soil, which multiplies by mitosis for as long as external foods, e.g., bacteria, are available. Upon food deprivation, however, starving cells initiate a developmental program that includes cell aggregation [7, 8]. The cell aggregate undergoes a series of morphogenetic changes to form a migrating pseudoplasmodium (slug) that eventually develops into a fruiting body, consisting of a mass of spores and a supporting stalk. The various developmental capabilities of *Dictyostelium* show that the organism has developed several solutions for life in the severe and variable soil environment. *Dictyostelium* amoebae have three choices (spore, microcyst, or macrocyst formation) open to them when faced with starvation. At least some species can form microcysts, in which each cell creates a thin cellulosic coat and undergoes other changes to prepare it for a short dormancy [9]. Whereas, macrocyst formation is recognized as part of the sexual cycle [10-12]. Incidentally, there is no report of microcyst formation under the culture conditions used, so far, for *Dictyostelium purpureum* (Dp), which was used as the host cell in the present study [9].

In this study, we used the model organism *Rhodobacter sphaeroides* as one of the photosynthetic bacteria supplied for ingestion by Dp-cells. This purple nonsulfur bacterium is widely distributed in soil and water and undertakes many processes, including assimilation, decarboxylation, nitrogen fixation, etc., depending on the environmental conditions. *R. sphaeroides* performs anoxygenic photosynthesis and, usually, nitrogen fixation and proton release using light energy from the sun. Because these bacteria are also able to extensively metabolize organic acids, amino acids, carbohydrates, etc., to obtain reducing power, the best growth conditions are anaerobic phototrophy (photoheterotrophic and photoautotrophic) in the presence of light and aerobic chemoheterotrophy in the absence of light [13].

For the second photosynthetic bacterial food source, we chose the unicellular *Synechocystis* spp. PCC 6803 that is systematically the cyanobacterium, as it has a globular shape (ca. 2 μm in diameter) but does not form a pair of long beads. The total length of the genome is 3,573,470 bp [14], and after our preliminary experiment its morphogenetic characteristics allow it to be phagocytosed by Dp-cells, although they are somewhat too large for their effective capture, resulting in a considerably slower host Dp-cell growth rate. The current oxygen concentration in the earth's atmosphere is thought to largely result from photosynthesis as performed by plants and algae, initially evolved more than a billion years ago from ancestral cyanobacteria, which acquired photosystem I and II as light capture devices capable of performing oxygenic photosynthesis [15]. Thus, cyanobacteria contain chlorophyll a and phycobilin as auxiliary photosynthetic pigments, both of which provide a blue coloration [16]. It has been hypothesized that cyanobac-

teria may have achieved symbiosis with mitochondria-containing eukaryotes, followed by their eventual transformation into the plant organelles known as chloroplasts [17-19].

The purpose of this research was to experimentally induce autotrophic organisms from heterotrophic Dp-cells in the laboratory by force-feeding them with the two types of photosynthetic bacteria, in order to illustrate the processes that probably occurred in ancient times. We report here other interesting findings obtained during the course of this work and discuss their evolutionary significance, with special emphasis on a possible mode of heterotrophy to autotrophy conversion that may have played out in the primordial era.

2. MATERIALS AND METHODS

2.1. Cell Strains and Growth Conditions

Dictyostelium purpureum 4-NI-20 (wild-type) was used as a heterotrophic host cell and grown with *Klebsiella aerogenes* on 3LP (0.3% lactose, 0.3% Bacto-peptone in 1.5% Bacto-agar). To create autotrophic cells from host Dp cells, a small number of Dp spores (5 μl in 20 mM phosphate buffer, pH 7.0) were placed at the center of inorganic agar on which *Rhodobacter sphaeroides* had been uniformly spread. The red photosynthetic bacterial suspension of *R. sphaeroides* was purchased from the EM Laboratory (Shizuoka, Japan). The green photosynthetic bacterium, *Synechocystis* spp. PCC 6803, was kindly supplied in a culture solution by Dr. E. Suzuki (Akita Prefectural University). A cell suspension (10 ml) of *R. sphaeroides* was centrifuged for 8 min at 8000 g and 4˚C to precipitate, and the resulting pellet was suspended in ca. 250 μl of sterilized water. A cell suspension (10 ml) of *Synechocystis* was centrifuged for 5 min at 5000 *g* and 4˚C to precipitate, and the resulting pellet was processed as for *R. sphaeroides*. This was followed by uniform plating of the dense cell suspensions on 1.5% inorganic agar (Bacto-agar dissolved in distilled water, BG-11 medium [GIBCO], or 20 mM Na/K-phosphate buffer, pH 7.0) in plastic Petri dishes (9 cm in diameter) and semi-drying by evaporation. Subsequently, an aliquot (5 μl) of Dp-cell suspension was placed at the center of the agar plate and incubated at 22˚C under about 12-h light (ca. 1450 lux on the agar surface) and about 12-h dark conditions, unless otherwise noted. During culture, the Dp cells engulfed the surrounding bacteria by phagocytosis and grew by spreading outward while expanding the forefront of growth. Photographs of cell morphology were taken under a stereo-, phase-contrast-, confocal or fluorescence microscopes.

2.2. Calcofluor White Stain

In order to detect the existence of cell walls, cells were washed twice suspended in 20 mM phosphate buffer (pH 7.0), and placed on a clean glass slide. Subsequently, one drop (100 μL) of Calcofluor White Staining Solution was added to the sample. After 20 min of incubation in a moisture chamber at room temperature, the slide was covered with a clean coverslip, and observed under a fluorescence microscope using UV light.

2.3. Electron Microscopic Procedures

Various types of cells and cell masses were fixed in 1% solution of OsO_4 dissolved in the standard salt solution (BSS) for 20 min at room temperature, as described before [20]. In another fixation, cells and cell masses were first fixed in 2% solution of glutaraldehyde dissolved in 20 mM PIPES buffer (pH 7.0) for one hr at room temperature and post-fixed in 1% solution of OsO_4 as described above after careful washing in 20 mM PIPES buffer (pH 7.0). After dehydration of the fixed samples in a series of ethanol, specimens were embedded in Epoxy resin. Ultrathin sections (60 - 80 nm thick) were cut with a Reichert Ultracut S. The sections were stained with lead citrate and were observed with a Hitachi H-500.

2.4. DAPI- and MitoTracker-Green-Stains of Cells

Cell masses grown on 1.5% non-nutrient agar were scraped off from the agar surface by a bacterial

spreader, and suspended in 1 ml of 20 mM Na/K-phosphate buffer, pH 7.0, at a density of ca. 1×10^6 cells/ml. Then, 5 µl of 1 µM Mitotracker stock solution in DMSO was added to 100 µl of the cell suspension, and vortexed vigorously. The cell suspension was placed on a cover-slip. After incubation of 30 min in a wet-chamber at 22˚C, the sample was washed three times with 20 mM Na/K-phosphate buffer, pH 7.0, dipped in ice-cold absolute methanol, and fixed for 10 min. Subsequently, 100 µl of DAPI staining solution (10 µg/ml DAPI in 20 mM Na/K-phosphate buffer, pH 7.0) was added, and incubated for further 3 hrs at 22˚C. The cover-slip was washed three times with the Na/K-phosphate buffer, pH 7.0, and observed under a fluorescent microscope (Zeiss, Switzerland, Model Axioscope A1).

2.5. Detection of Chlorophyll Fluorescence

Living Dp-green cell masses and host *D. purpureum* cells (as control cells) were separately placed on glass base dishes (Iwaki) and observed under a confocal microscope (Fluoview FV 1000, Olympus, using an excitation wavelength (440 nm) and an emission wavelength (620 nm) to detect chlorophyll fluorescence. Differential interference contrast (DIC) images of the respective cells were photographed under a DIC microscope.

2.6. Genetic Analysis of Partial 5.8S rRNA Gene

Vegetative cells of Dp and *D. discoideum* Ax-2 were harvested, placed into 20 mM Na/K-phosphate buffer, pH 7.0, and washed by three centrifugations. The Dp-green cell masses incubated on 1.5% inorganic agar were also collected and washed in the buffer. Genomic DNA was isolated from the washed cells with the DNeasy Tissue Kit (Qiagen, Germany). PCR was performed by following either the protocol used for the amplification of partial sequences of 5.8S rRNA of Dictyostelids [20] or that of the Dd-MRP4 gene whole sequence in *D. discoideum* [21]. The DNA sequences of primers used for *Dictyostelium discoideum* mitochondrial protein S4 (*Dd-mrp*4*;* MtS4) and 5.8S rRNA (Dic_5.8S_rRNA) are as follows:

Dic_5.8S_rRNA_F: GAGGAAGGAGAAGTCGTAACAAGGTATC
Dic_5.8S_rRNA_R: GCTTACTGATATGCTTAAGTTCAGCGGG
MtS4_FH3: TAGGATCCATGAGACAACGAAAAAATGTGACAAAATTT
MtS4_RB1: CGAAGCTTTTATCTTAGTCTTTTATATTTCTTTAATAAAG

PCR cycle conditions are as follows: denaturing step at 94˚C for 5 min, followed by 30 cycles of 94˚C for 1 min, 55˚C for 1 min and 68˚C for 1 min.

2.7. Genome Wide Analysis of Dp-Green Cell Masses

Dp-green cells were grown on 1.5% 1/5 SM agar plates, feeding with *K. aerogenes*. About 1×10^7 cells were collected and washed in 20 mM Na/K-phosphate buffer, pH 7.0. Genomic DNA was isolated from washed cells with DNeasy Tissue Kit (Qiagen, Germany). Isolated genomic DNA was analyzed by MiSeq Microbiological Genome Draft Analysis Service provided by FASMAC, Japan. Retrieved genomic scaffold data were analyzed with Mole-Blast (NCBI, NIH, USA).

3. RESULTS

3.1. Formation of Microcysts from *D. purpureum* Cells by Forced Feeding of Photosynthetic Bacteria

When wild-type Dp amoeboid cells were incubated with *K. aerogenes* as a food source on semi-nutrient (3LP) agar plates, they proliferated rapidly and phagocytosed the bacteria (**Figure 1(A)**). Upon exhaustion of the bacteria, the starving cells differentiated to acquire aggregation-competence and constructed multicellular structures. The cell mass migrated to form a cellular stalk at the tip (**Figure 1(B)**) and, finally, differentiated into a fruiting body with a mass of spores at the top.

As the first step to create autotrophic cells from host Dp cells, a small number of Dp spores were incubated with *R. sphaeroides* (see Materials and Methods section for detail). Henceforth, the first inoculated

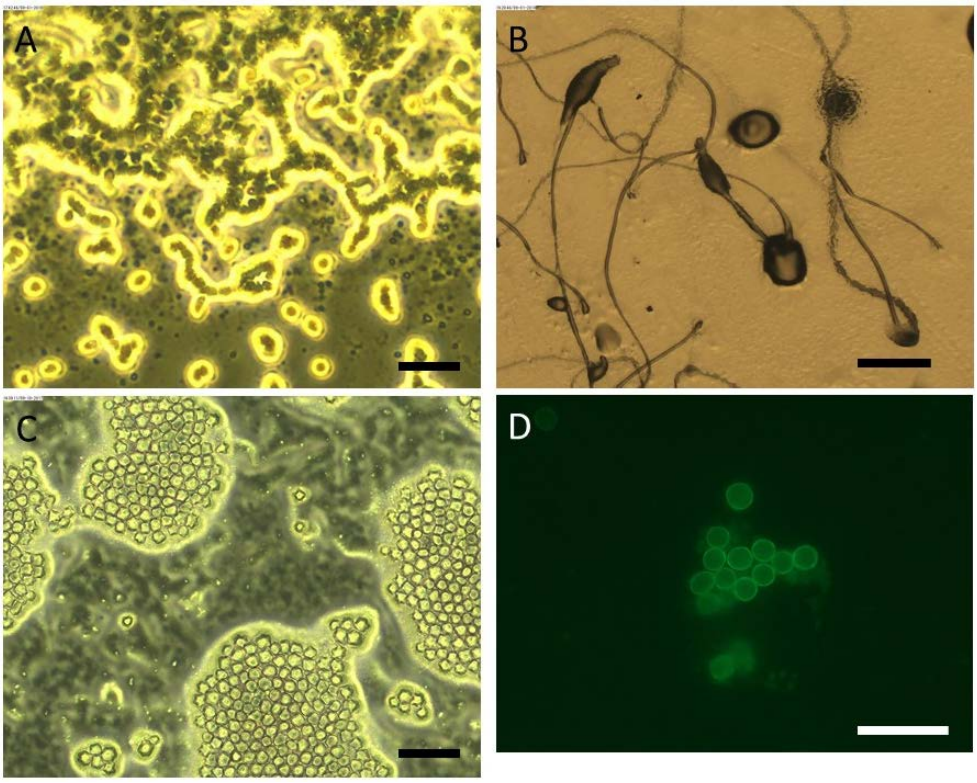

Figure 1. Differences in morphology during growth and subsequent morphogenesis of *Dictyostelium purpureum* depending on the type of food provided during the vegetative phase. (A) Phase-contrast microscope image of vegetative *D. purpureum* cells growing after feeding on *Klebsiella aerogenes*. Bar, 50 μm. (B) Morphogenesis of *D. purpureum* cells after consuming food. Starved cells aggregated and migrated (arrow) as pseudoplasmodia to eventually form fruiting bodies consisting of spores and a supporting stalk. Bar, 1 mm. (C) Sheet-like clusters of microcysts formed by forced feeding with *Rhodobacter sphaeroides*, instead of *K. aerogenes*, and subsequent starvation. The sample was collected Bar, 50 μm. (D) Fluorescence microscope image of the cell cluster. The outer-most surface of each round cell is stained with calcofluor, showing the presence of cellulose and/or chitin in the wall. Bar, 50 μm.

cells are referred to as the 1st transferred cells (1st Dp cells) for convenience. During incubation, the 1st Dp spores germinated, actively engulfed as amoeboid cells the surrounding bacteria by phagocytosis and multiplied and spread outward while expanding the forefront of growth, which reached the outermost region of the agar plate (diameter, 9 cm) within 5 days of incubation at 22˚C. Starving cells located at and near the inoculation spot exhibited normal morphogenesis to form fruiting bodies. However, the cells located further away failed to aggregate and formed sheet-like cell clusters, as shown in Figure 1(C), consisting of somewhat rounded cells.

The surface of each rounded cell was stained with calcofluor (Figure 1(D)), which that binds to cellulose and/or chitin in the cell wall, and was considered a microcyst, which has not been reported before in *D. purpureum*. After 7 days of incubation, the outermost cells were transferred in droplets to the center of inorganic agar on which red photosynthetic *R. sphaeroides* had been uniformly spread, and incubated for another 7 days as 2nd Dp cells. The cells at the outermost region should have been those that had divided the most during the course of the incubation, while phagocytosing the bacteria. As was expected, the 2nd Dp cells grew and divided while actively phagocytosing the bacteria, and most did not exert normal mor-

phogenesis after starvation but formed clusters of microcysts instead of autotrophic cells. The 3rd Dp cells were found to lose their morphogenetic ability after starvation, although their vegetative growth and proliferation in the presence of bacteria were almost normal. Despite this situation, we tried to obtain autotrophic cells by repeated transfer of the Dp cells. Unfortunately, however, no signs of autotrophy were recognized, even in the 21st Dp cells incubated for ca. 5 months.

3.2. Creation of a Unique Autotrophic Organism with a Dark Brown Color

In the second attempt, we forced the 21st Dp cells to ingest another species of photosynthetic bacteria, the cyanobacterium *Synechocystis* spp. PCC 6803. When the 21st Dp cells were transferred to the center of inorganic agar (1.5% agar containing BG-11 medium or 20 mM Na/K-phosphate buffer, pH 7.0) on which *Synechocystis* had been uniformly spread, they grew slowly while feeding on the bacteria, and the forefront of growth reached the outermost region of the 9-cm agar plate after 7 - 8 days of incubation at 22˚C. The outermost cells were again spot-inoculated onto *Synechocystis*-spread agar, as in the case of *R. sphaeroides*, and incubated for 7 days. Although autotrophic cells did not appear in the 2nd transferred population, notable results were obtained by chance when the 3rd transferred cells were incubated and abandoned for 53 days: a considerable number of dark-brown cell masses formed near or at the center of the agar plate, as shown in **Figure 2(A)**. From their morphological and behavioral characteristics (**Figure 2(B)**), they seemed to be formed by autotrophic growth, and this was proven in the next stage of the study.

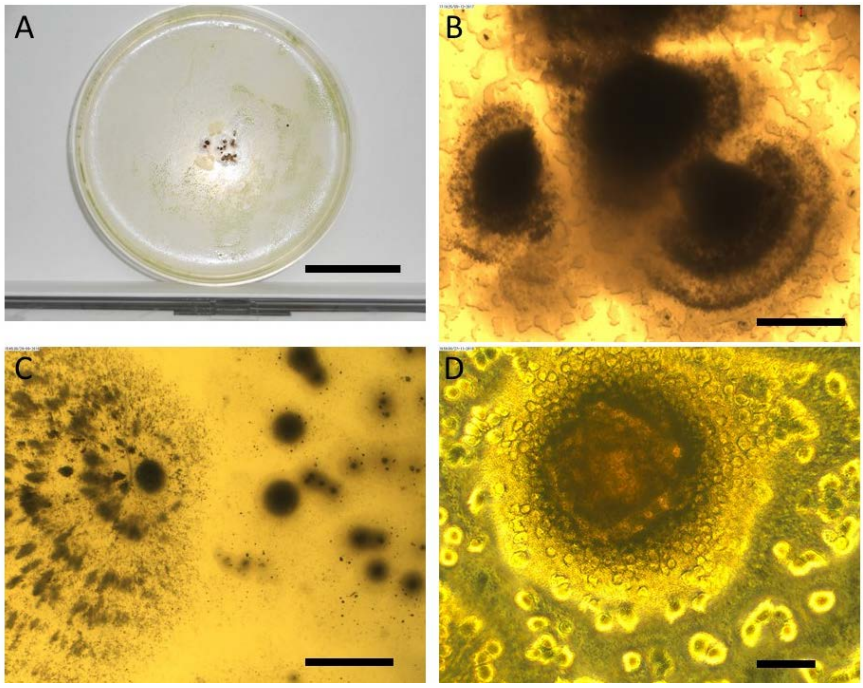

Figure 2. Dark-brown-cell masses formed by forced feeding with *Rhodobacter shaeroides* and, subsequently, *Synechocystis*, and their autotrophic growth without a food source. (A) Dark-brown-cell masses formed in the central area of 1.5% agar plates after about 6 months of forced feeding with *R. sphaeroides* and subsequent feeding with *Synechocystis*. Bar, 3 cm. (B) Enlarged image of the dark-brown-cell masses. Bar, 1 mm. (C) Distribution pattern of brown-cell masses formed after 14 days of autotrophic growth without a food source. In addition to the periodic light-brown distribution pattern (left side), a considerable number of globular brown-cell masses formed remote islands (right side). Bar, 5 mm. (D). Phase-contrast microscope image of a dark-brown cell mass and surrounding amoeboid cells. 50 μm.

Green-colored autotrophic cell masses had not been obtained by the repeated culture of host Dp cells with *Synechocystis* alone for about 8 months. Instead, Dp cells cultured with *Synechocystis* rapidly lost their morphogenetic ability to form fruiting bodies after starvation and became microcysts, as in the case of the culture with *R. sphaeroides*.

3.3. Developmental Characteristics of Unique Autotrophic Organisms

To confirm that the formation of the dark-brown cell masses described above was due to autotrophic growth through photosynthesis, a part of the mass was aseptically transferred to inorganic agar (typically, 1.5% agar dissolved in BG-11 medium or 10 mM Na/K-phosphate buffer, pH 7.0), using a sterilized toothpick or platinum loop and were incubated without a food source like bacteria. This replanting of cells was performed aseptically under a stereomicroscope on a clean bench. As a result, a considerable number of dark-brown regions with a unique distribution pattern were formed within 10 days of incubation (**Figure 2(C)**). That is, in addition to a stripe pattern with an underlining pattern of small dots (**Figure 2(C)**, left side), a number of globular dark-brown regions formed as small islands (**Figure 2(C)**, right side). At the earliest developmental stage, many amoeboid cells were produced around the spherical dark-brown mass, as shown in **Figure 2(D)**. Free-living amoeboid cells, some of which were in the process of cell division, were observed on the exterior of the cell masses. When observed in detail, the central dark-brown mass and the surrounding dark-brown islands were found to be connected to each other by a thin multinucleate plasmodium that spread widely and radially as a very thin layer from the center. The multinucleate plasmodium was found to be critical for autotrophic growth, as described later. Importantly, a significant number of amoeboid cells were constructed in a budding-manner from the thin multinucleate plasmodium. Incidentally, we found that the first dark-brown cell masses could live for a long time, as they retained the ability to form the autotrophic organism, even when left unattended for at least 3 years at 22˚C.

During successive planting of the dark-brown cell masses without a food source, some of the cell masses spontaneously transformed into green-colored masses (referred to as Dp-green cell masses for convenience), as shown in **Figure 3(A)**. Many amoeboid cells were produced from the masses (**Figure 3(B)**). The Dp-green cell mass also formed a multinucleate plasmodium that spread radially outward from the center of the Dp-green mass, as the case in the dark-brown cell mass. A significant number of amoeboid cells were constructed from the tip (**Figure 3(C)**, **Figure 3(D)**, **Figure S2(B)**) or the intermediate region of a green multinucleate plasmodium (**Figure 3(B)**, **Figure S1**), possibly via the self-organization of Dp-derived nuclei, mitochondria, red pigments (probably derived from *Rhodobacter*), and green pigments (possibly derived from *Synechocystis*) that were present as granular or lamella structures (**Figure S1**). A thin reticulated multinucleate plasmodium formed at the outermost peripheral region, and apparently cell-like protrusions sometimes formed in a process similar to budding (**Figure 3(C)**, **Figure S2(B)**). As a result, many amoeboid cells were produced and migrated over the substratum from the outermost area of the plasmodium (**Figure 3(D)**, **Figure S2(B)**). Importantly, we found that the outermost region of the green plasmodium, apparently without amoeboid cells, had the ability to generate Dp-green cell masses when transferred to a new inorganic agar plate and cultivated without a food source. In the nuclear regions of Dp-green cells, red and green pigments derived from *Rhodobacter* and *Synechocystis*, respectively, were often observed, as shown in **Figure S1**.

Cells that could not become green cell masses gradually become light-brown cell masses in which most of *Synechocystis*-derived green granules were missing. At the earliest developmental stage, the globular cell mass formed a cluster of protrusions with the appearance of small plant roots. Subsequently, a thin multinucleate plasmodium was formed, and some amoeboid cells were produced and released from the plasmodium, as shown in **Figure S2**. Interestingly, formation of the light-brown cell masses was formed even in the dark, and its property was stably retained in the process of further subculture. The highest growth rate of the green plasmodium was about three times higher than that of light-brown plasmodium: the rate of radial horizontal spread of the green plasmodium on agar was ca.15 μm/hr, while that of the light-brown plasmodium was ca. 5 μm/hr.

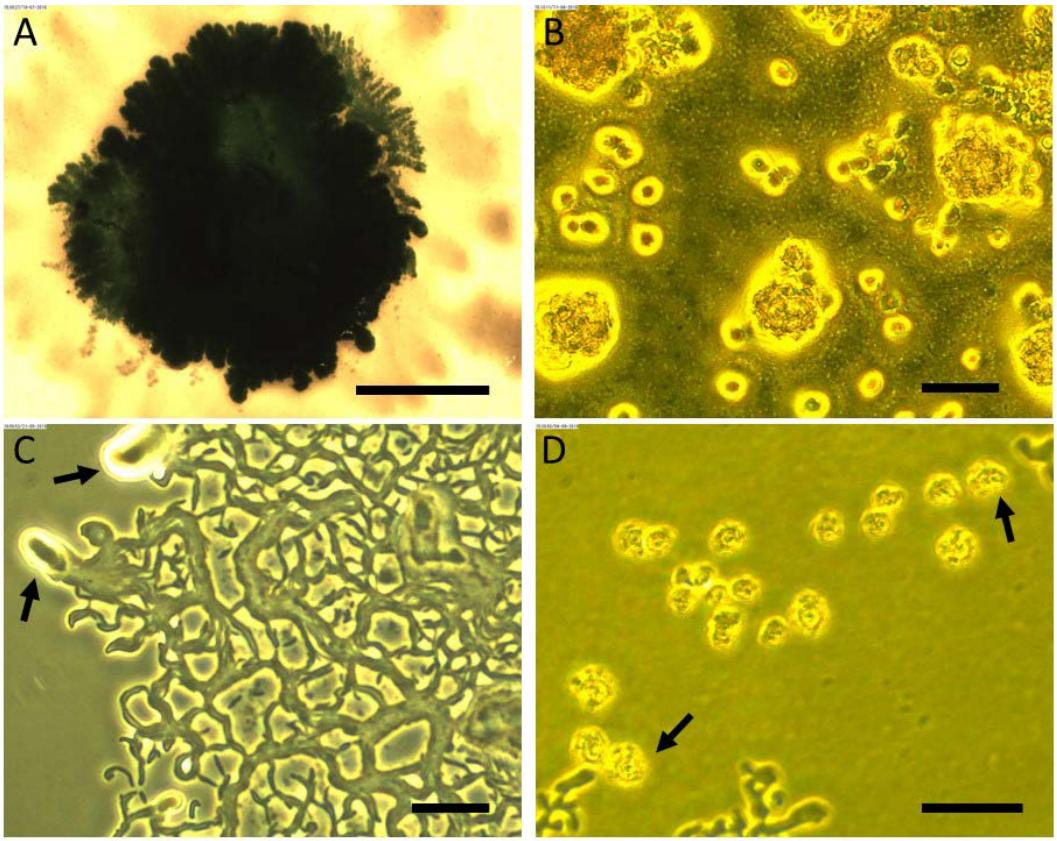

Figure 3. Morphology and behavior of Dp-green cell masses formed spontaneously from Dp-dark-brown cell masses. (A) Gross morphology of a green-cell mass formed by autotrophic growth of Dp-brown cells during culture. Bar, 2 mm. (B) Amoeboid cells near the center of the cell masses. Bar, 60 μm. (C) A thin reticulated multinucleate plasmodium in the outermost region. Two cell-like protrusions (arrows) formed from the leading edge of the plasmodium. Bar, 50 μm. (D) Amoeboid cells (arrows) that migrated outward by amoeboid movement from the leading edges. Bar, 80 μm.

When a small number of Dp-green or Dp-light-brown cell masses were transferred in droplets to the center of inorganic agar, on which *R. sphaeroides* or *Synechocystis* had been uniformly spread, and incubated for another 7 days, both of the cells failed to ingest temporally the microbes by phagocytosis for about two days and exerted autotrophic growth during the lag period. This was followed by heterotrophic growth, phagocytosing actively the external bacteria. When agar plates were spread with *Klebsiella aerogenes*, both the Dp-brown and Dp-green masses lost their ability to phagocytose for about 2 days of incubation: they exhibited autotrophic growth during this period and then began to proliferate, engulfing the *K. aerogenes*. This seems to indicate that once autotrophic traits were acquired, the cells did not need to feed on bacteria for their growth temporally. Importantly, however, the Dp-green masses that had proliferated in a heterotrophic pattern while engulfing *Synechocystis* after about 4 days of lag time eventually formed a sheet of microcyst-like cells after about 15 days of incubation. When a small number of the microcyst-like cells were transferred to a new inorganic medium and incubated without food, they grew autotrophically again. Incidentally, the lag-time of the first 4 days was temporally allowed only shortly after transfer from autotroph to heterotroph. Actually, the lag period time was no longer allowed when the heterotrophically grown Dp-green masses were transferred to a new plate on which *K. aerogenes* had been spread. Taken together, these results indicate that the Dp-green masses could grow heterotrophically, as

well as autotrophically, and so retained their basic genetic features required for autotrophic growth.

3.4. Fine Structures of the Green Plasmodium, Its Derived Amoeboid Cells and Host Dp-Amoeboid Cells

In the central region of a green multinucleate plasmodium, *Synechocystis*-derived bodies were predominantly present, and other structures such as *Rhodobacter*-derived bodies and Dp-derived mitochondria were also observed (**Figure S3** and **Figure 4** shows fine structures of the middle region of a green multinucleate plasmodium, in which a variety of organelle-like structures, including *Synechocystis*-derived bodies, *Rhodobacter*-derived bodies, and a cluster of structurally modified mitochondria were mainly visible. Surprisingly, however, it was found that the cell membrane of the multinucleate plasmodium and amoeboid cells was not retained by double fixation with glutaraldehyde and OsO_4 as well as by single fixation with OsO_4. Probably, the membrane structures of the created autotrophic plasmodium and amoeboid cells derived from it might be very fragile, thus resulting in failure of preservation of cell membrane systems during fixation and subsequent dehydration. The absence of small ribosome-like granules might be because these structures might be leaked from the plasmodium and amoeboid cells after the cell membrane was greatly damaged. Nevertheless, electron-dense membranes as observed in structurally modified *Synechocystis*, and structurally modified mitochondria were observed in the cytoplasm of the green plasmodium and amoeboid cells (**Figure 4**, **Figure S4**. The cell membrane structure was also scarcely noticed in the light brown plasmodium and amoeboid cells derived from it. Instead, a cluster of unique mitochondria was often observed in the light-brown plasmodium and amoeboid cells as well as in the green plasmodium and amoeboid cells. Interestingly, most of the modified mitochondria were found to be covered

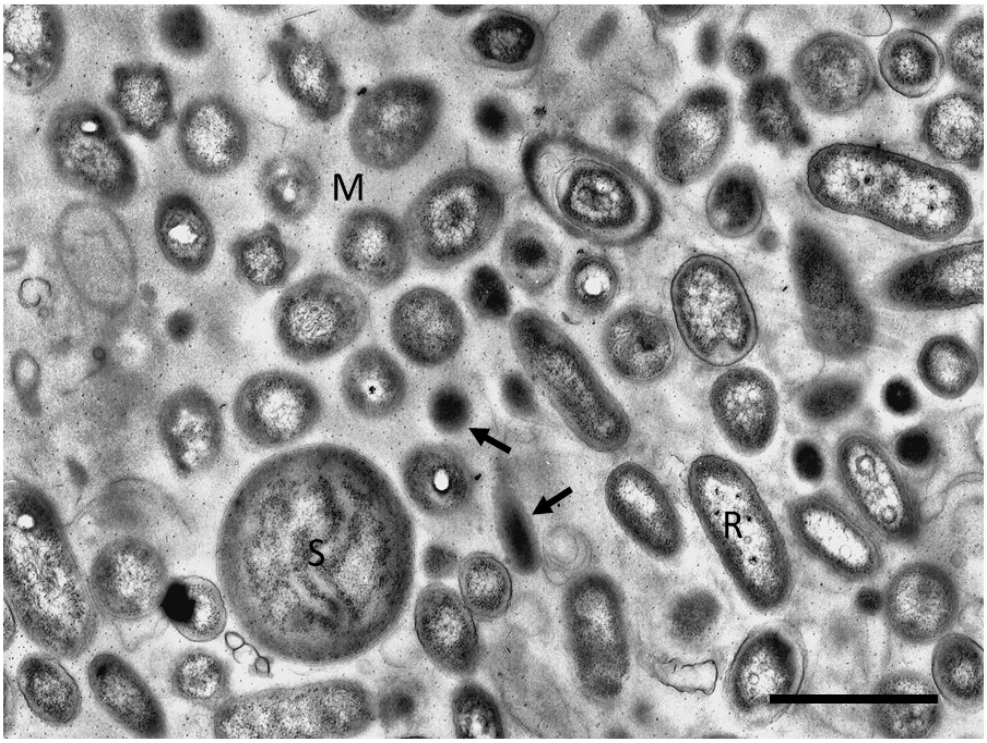

Figure 4. The fine structure of a multinucleate plasmodium located the peripheral site of a Dp-green cell mass. A variety of organelle-like structures, including *Synechocystis*-derived body (S), *Rhodobacter*-derived body (R), and a cluster of unique mitochondria (M), are visible. A considerable number of unidentified electron-dense bodies (arrows) are also seen. Bar, 1 μm.

with electron-dense membranes (Figure S4). The mitochondria seemed to correspond to those of host *D. purpureum* cells. In the case of host Dp-amoeboid cells, at least two kinds of mitochondria with different electron densities were observed, as shown in Figure 5. Such heterogeneity is rarely found in the population of *D. discoideum*-mitochondria [22]. In the cytoplasm of Dp-amoeboid cells shown in Figure 5, a considerable number of cavities without boundary membranes as observed in Golgi complexes and small vesicles were recognized. In addition, there is a limited part of cell membrane where the unit membrane structure is not so clear. These structural features are not found at least in *D, discoideum* cells [22]. Accordingly, it is possible that such vulnerabilities of the membranes in host Dp-cells may be passed on to the green plasmodium and amoeboid cells derived from it. The red and/or green pigments, as shown by the phase-contrast micrograph of Figure S1, seemed to correspond to the unique inclusion bodies present in the nuclear region of the plasmodium-derived amoeboid cells (see the EM image of Figure S4).

3.5. The Autotrophic Plasmodia and Their Derived Amoebae Contain a Considerable Number of Granules with *Synechocystis*- and/or *Rhodobacter*-Derived DNAs, in Addition to a Mass of Dp-Derived Mitochondria

The green plasmodium-derived amoeboid cells were stained with a mitochondria-specific fluorescent marker, MitoTracker Green, and the DNA-specific dye, DAPI, to examine the distribution of mitochondria and DNA-containing organelles, including cell nuclei, respectively. In a differential interference contrast micrograph of an amoeboid cell shown in Figure 6(A), an almost circular and non-granular area was

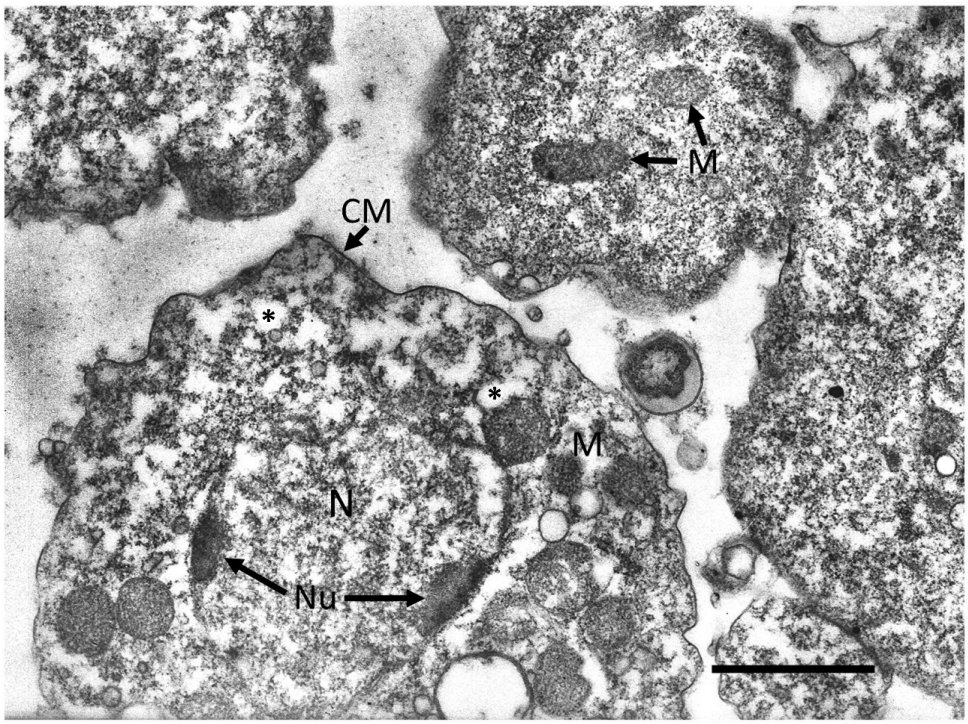

Figure 5. Ultrastructure showing *Dictyostelium purpureum* (Dp) amoeboid cells at the vegetative growth phase. In the nucleus (N), two nucleoli (Nu) are observed in contact with the nuclear membrane. In the cytoplasm, at least two kinds of mitochondria with different electron densities were observed, Also, a considerable number of cavities (asterisks) without boundary membranes as observed in Golgi complexes and vesicles are recognized. CM, cell membrane; M, mitochondria. Bar, 1 μm.

observed. From its shape, this area is regarded as the nuclear region. As expected from the electron microscopic observations, however, the cell nuclear regions were not stained with DAPI (Figure 6(B)), possibly because of leakage of DNA from the nucleus during fixation. On the other hand, the number of stained mitochondria was found to be much higher than that in parental *D. purpureum* cells (Figure 6(C), Figure S6). Figure 6(D) shows the merged image of DAPI-staining and MitoTracker Green-staining. The original green-colored granular stains were artificially converted to red in Figure 6(C) in order to merge with the DAPI-staining in Figure 6(B). Numerous pink granules with mitochondria with DNA were observed, in addition to and a small number of blue granules containing probably *Synechocystis*- and/or *Rhodobacter*-derived DNAs (Figure 6(D)). In (D), three distinct yellow granules were observed near the nuclear region, beside the pink and blue granules. Since yellow is a merged color of green and red, there are the possibility that a small number of green-colored granules will be present in the amoeboid cells. For comparison, the staining patterns of host *D. purpureum* cells with DAPI and MitoTracker-Green are shown in Figure S5.

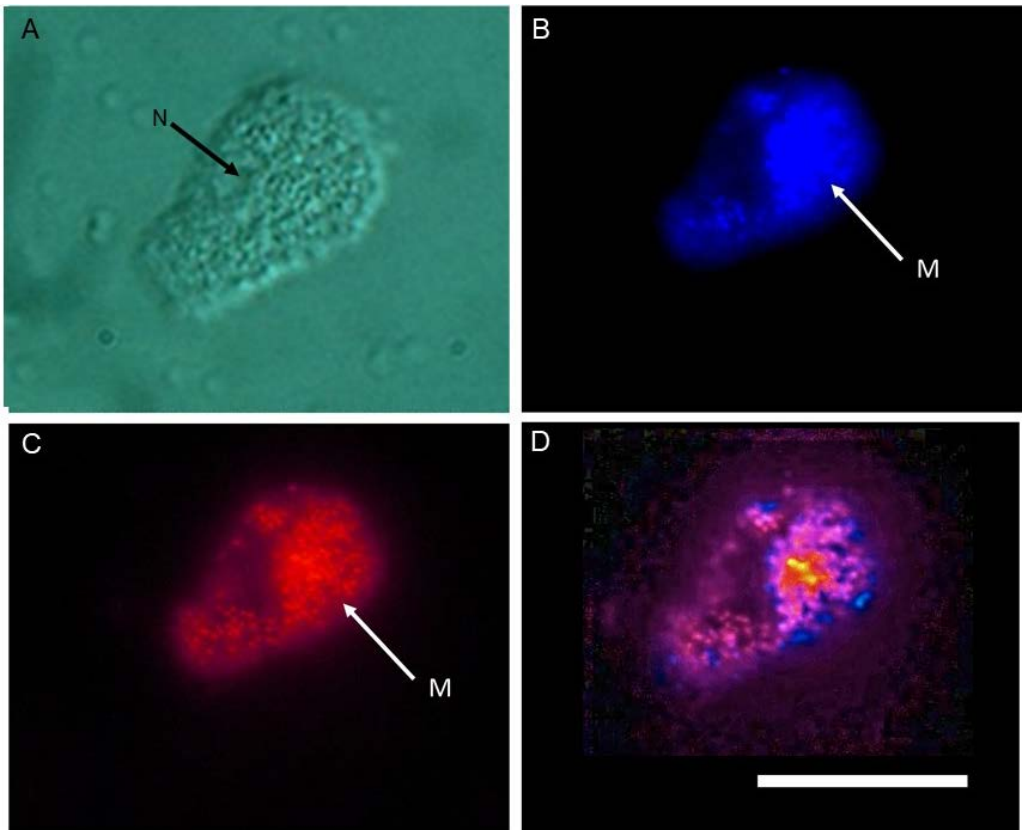

Figure 6. Staining of an amoeboid cell derived from the green plasmodium with DAPI and MitoTracker-Green. (A) DIC (differential interference contrast) microscopic image. N, nuclear area. (B) DAPI-staining image of the interference contrast microscopic image. N, nuclear area. N, nuclear area. (B) DAPI-staining image of the same region with (A). M, cluster of mitochondria. (C) MitoTracker-Green-stained cells of the same region as (A). M, cluster of mitochondria. (D) The merged image of DAPI-staining (B) and MitoTracker-Green-staining (C). The original green-colored granular stains with MitoTracker-Green were artificially converted to red in (C) in order to merge with the DAPI-staining in (B). Note numerous pink granules (mitochondria with DNA) and a significant number of blue granules containing probably *Synechocystis*-derived DNA. Beside the pink and blue granules, three distinct yellow granules are observed near the nuclear region. Bar, 10 μm.

3.6. The Green Plasmodium Has a Significant Number of Granules with Chlorophyll Fluorescence

To know if the green plasmodium and its derived amoeboid cells have fluorescence with chlorophyll, they were observed under a confocal microscope, using excitation wavelength of 440 nm and emission wavelength of 620 nm (Figure 7(A), Figure 7(B)). As a result, it was found that the plasmodium contains a significant number of granules with chlorophyll fluorescence (Figure 7(B), Figure 7(C)), while that many of the amoeboid cells have no chlorophyll fluorescence-positive granules in the cytoplasm with an exception that a small number of cells have one or two red granules with chlorophyll fluorescence (Figure 7(C), arrow). As expected, host Dp-amoeboid cells that had been heterotrophically grown, feeding on *K. aerogenes*, had no chlorophyll fluorescence-positive granules in the cytoplasm (Figure 7(D), Figure 7(E)). Figure 8 shows excitation wavelength dependency of chlorophyll fluorescence in the area of a green plasmodium and amoeboid cells derived from it. From the fluorescence spectrum, it is evident that the maximum value (relative fluorescence emitted by 440 nm of wavelength) is around 680 nm (Figure 8), which is

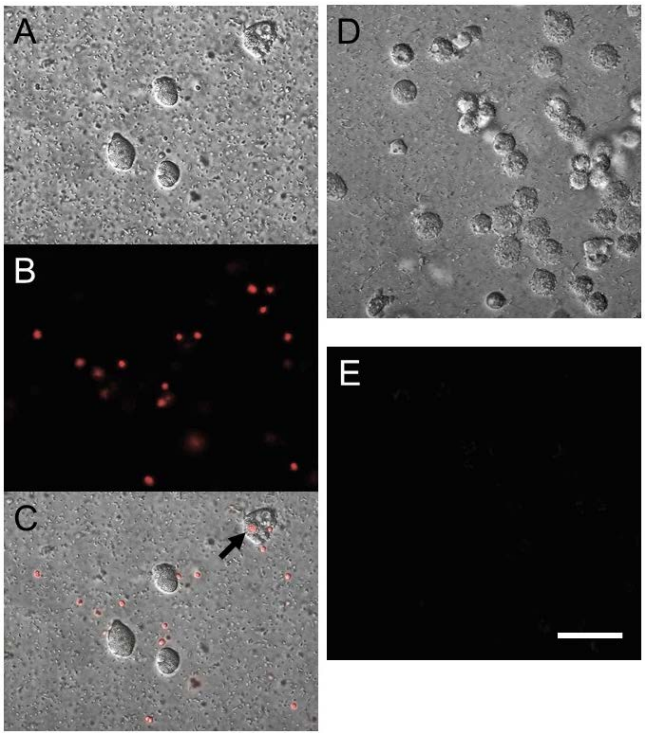

Figure 7. Microscopical detection of chlorophyll fluorescence in the green multinucleate plasmodium and its derived amoeboid cells. An autotrophically growing green plasmodium and its derived amoeboid cells were observed under a confocal microscope using an excitation wavelength (440 nm) and an emission wavelength (620 nm) to detect chlorophyll fluorescence. (A) A DIC image of the green plasmodium and amoeboid cells. (B) A photograph of the same field of view with (A), taken under the confocal microscope. The structures with chlorophyll fluorescence are shown as red granules. (C) A merged image of (A) and (B). It is evident that the green plasmodium has a considerable number of red granules with chlorophyll fluorescence. Note that many of amoeboid cells are devoid of red granules, though a few cells contain one or two red granules in the cytoplasm (arrow). (D) A DIC image of host Dp-cells grown heterotrophically with *Klebsiella aerogenes*. (E) As expected, chlorophyll fluorescence is never observed, indicating the absence of photosynthetic organelles like chloroplasts. Bar, 50 μm.

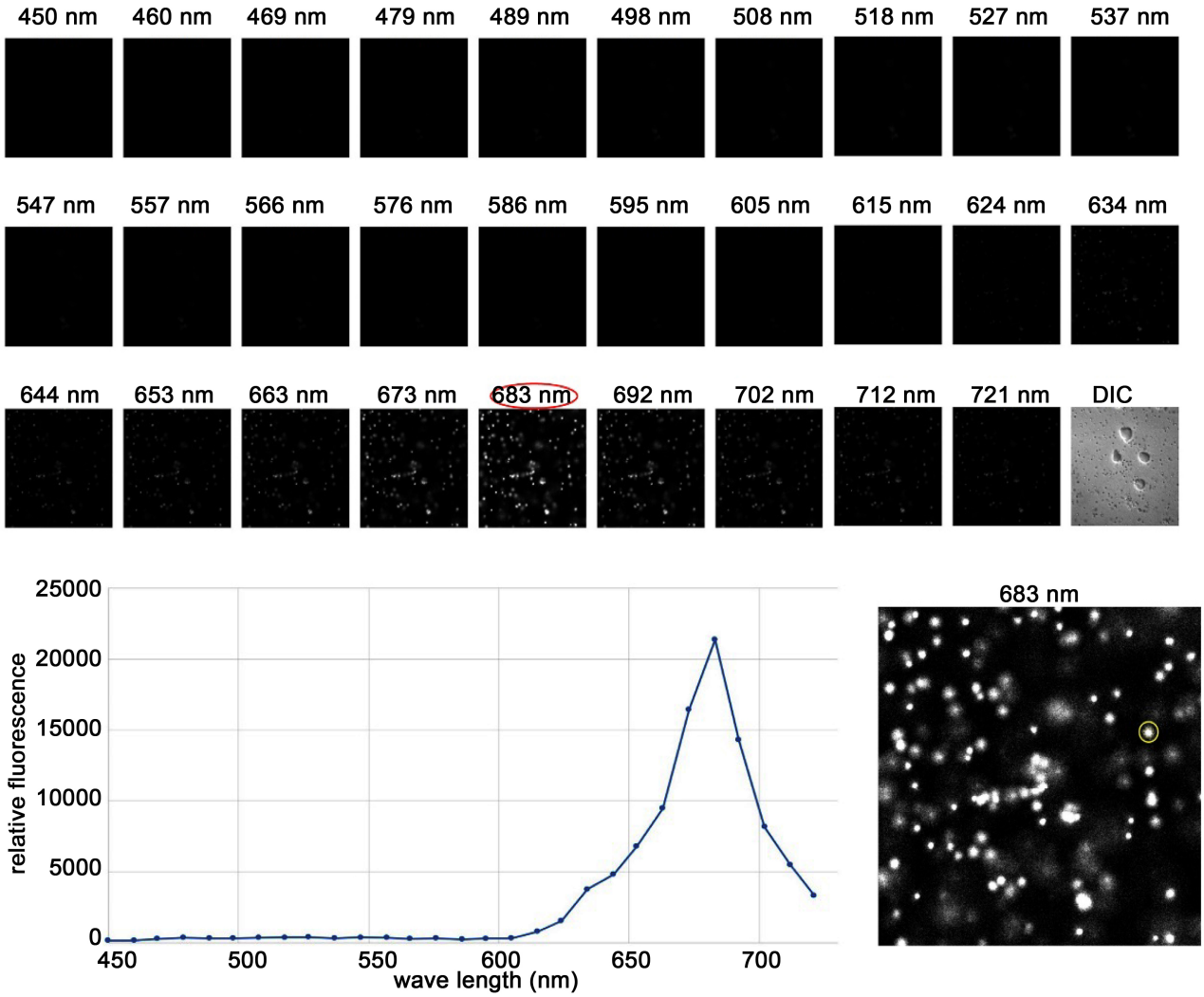

Figure 8. **Chlorophyll fluorescence spectrum depending on emission wavelength in a green plasmodium and its derived amoeboid cells. Upper figures: Total 29 images of the same sample excited by light with a wavelength of 440 nm. The fluorescein emission at the wavelength indicated on the respective figure was photographed. The photo on the far right of the third row is a DIC-image of the selected sample area. The photo on the bottom right is an image taken at 683 nm of emission wavelength. Many bright and small particles (possibly *Synechocystis*-derived granules) are observed. On the lower left graph, the emission wavelength (horizontal axis)-dependency of relative fluorescence (vertical axis) is shown: the maximum fluorescence value emitted by 440 nm of wavelength being attained around 680 nm of emission wavelength. The measurement of fluorescence emission was done, focusing on a small circle shown in a lower right magnified panel.**

a typical spectrum of chlorophyll fluorescence. According to continuous observation of the green plasmodium and amoeboid cells derived from it under a DIC-microscope, the amoeboid cells were found to be located on the underside of the plasmodium and perform an active amoeboid movement on the surface of the plasmodium. Here it is important to note that the amoeboid cells never take up the constituents of the green plasmodium by phagocytosis. Therefore, it is almost unlikely that the amoeboid cells may ingest the green plasmodium (a kind of biofilm) as a food source to support heterotrophic growth.

3.7. The Genetic Background of the Green Multinucleate Plasmodium and Its Derived Amoeboid Cells

The genomic DNAs of parental *D. purpureum* cells, *D. discoideum* cells, and green multinucleate plasmodium containing amoeboid cells were isolated and amplified by PCR using 5.8S rRNA (ribosomal RNA (a non-coding RNA component of the large subunit of the eukaryotic ribosome) primers commonly used for phylogenetic studies of *Dictyostelium*. A single amplicon of a partial 5.8S rRNA sequence was amplified from the parental *D. purpureum* (**Figure S6**, Lane 5) and *D. discoideum* (**Figure S6**, Lane 4) genomic templates. However, several amplicons were observed with the genomic template of Dp-green cell masses (**Figure S6**, Lane 6). In addition, the DNA sequences similar to the *D. purpureum* genome were not found in the strongest band of the Lane 6. When the genomic template of parental *D. purpureum* cells was amplified with PCR using primers for Dd-MRP4 (mitochondrial ribosomal protein S4 of *D. discoideum*), a single, weak band was visible (**Figure S6**, Lane 2), whereas the genomic template of parental *D. discoideum* cells produced a single, strong band (**Figure S6**, Lane 1). In contrast, when green plasmodia containing amoeboid cells were used for PCR with the Dd-MRP4 primers, no bands were observed (**Figure S6**, Lane 3), indicating that the sequences comparable to Dd-MRP4 were either lost or partially mutated in the green plasmodia containing amoeboid cells and also in host *D. purpureum* cells.

For some of the amplifications, two amplicons were produced, each of which was identified as being DNA sequences derived from *Rhodobacter* and *Synechocystis*, suggesting that the two amplicons might be the result of the miss-priming of primers to the template (**Figure S6**. Lane 6). Parental *D. purpureum* 5.8S rRNA was not identified in these amplicons. Green plasmodium containing amoeboid cells were also analyzed with MiSeq genome wide sequencing. Curiously, assembled data were not identical with parental Dp cells' genome, and seemed to contain many kinds of bacterial genome fragments. Although some of them were identified as *Synechocystis*- and *Rhodobacter*-genomes, most genome fragments were found to be similar to those of gram-negative aerobic bacteria such as *Chitinophaga* and *Brevundimonas* (data not shown). Unexpectedly, in the above MiSeq genome wide sequencing analysis some fragments were found that slightly resembled the gene sequence of free-living *Acanthamoeba*. Possible interpretation of these strange data will be discussed in the next section.

4. DISCUSSION

Here, we discuss the mechanisms underlining the conversion of heterotrophy to autotrophy. Some types of photosynthesis involve the generation of oxygen, such as in green plants, and others involve the oxidation of H_2S and other substances, such as in purple bacteria. It is estimated that the majority of organic matter and atmospheric oxygen that currently exists were produced by photosynthesis. The emergence of autotrophic eukaryotes was a crucial step, allowing a variety of organisms to thrive as they do today; its establishment required two steps of intracellular symbiosis between two types of organelles: respiratory mitochondria and photosynthetic apparatuses like chloroplasts. In this connection, although such groundbreaking endosymbiosis is believed to have been established by about 100 million years ago [23], there has been no way to reproduce or demonstrate the events that occurred during the establishment of primary endosymbiosis. The precise nature of the host cell that partnered with the endosymbiont containing chloroplasts remains to be an open question. However, it is of interest to know how and how often plastids such as chloroplasts moved one eukaryote to another during algal diversification through the primary, secondary, and tertiary endosymbiosis [24]. Hence, in the present work, we tried to experimentally create autotrophic organisms from heterotrophic amoeboid cells lacking photosynthetic capacity. For this purpose, wild-type Dp cells were used as heterotrophic host cells, and two kinds of photosynthetic bacteria, *R. sphaeroides* and *Synechocystis* spp. PCC, were used as food sources for the Dp-cells.

Both the autotrophic Dp-light brown cell masses and the Dp-green cell masses were experimentally induced by two-step force-feeding with *R. sphaeroides* followed by *Synechocystis* spp. PCC 6803. In connection with this, it is most likely that the forced feeding and endosymbiosis of the heterotrophic Dp-cells with *R. sphaeroides* seem to be prerequisites for the creation of the autotrophic organisms, as we have not

succeeded in producing autotrophic Dp-dark brown, Dp-green and Dp-light brown cell masses by force-feeding cells with *Synechocystis* only, despite many, long-term cultures. The key to autotroph formation is considered to be the selection of the appropriate host cells (*Dictyostelium*) and the order of feeding with *R. sphaeroides* followed by *Synechocystis*. In other words, the findings presented here strongly suggest that endosymbiosis of the green pigment gene derived from *Synechocystis* may be required for the creation of photoautotrophic organisms from Dp-cells, coupled with the incorporation of the red pigment gene (derived from *R. sphaeroides*) into host Dp-cells. In other words, the endosymbiont *R. sphaeroides* was probably necessary to facilitate the establishment of the photoautotrophic Dp-green plasmodium. In the condition that *Synechocystis*-derived structures are retained in amoeboid Dp-cells without being digested, its photosynthesis is likely to cause significant damage to the amoebae using reactive oxygen species. Therefore, it will be necessary to possess the structure of alleviating and inhibiting photosynthetic oxidative stress in order to make photosynthetic devices such as *Synechocystis* coexist stably in eukaryotic cells. In this connection, it is possible that Dp-cells pre-cultured with *Rhodobacter* may have effect of relieving photosynthetic oxidative stress by engulfed *Synechocystis*, thus resulting in its successful endosymbiosis.

The difference between the Dp-light brown and Dp-green cell masses seems to be principally a result of the quantitative or qualitative differences in the red and green pigments contained in the two types of cell masses. Importantly, the Dp-light brown cell mass was produced in a light-independent manner, as they formed even under completely dark conditions. Actually, the Dp-light brown plasmodium as well as the amoeboid cells derived from it were mostly missing green granules derived from *Synechocystis*. This is in contrast to the Dp-green plasmodium that needs light to efficiently grow in an autotrophic fashion. Thus it is possible that the Dp-light brown plasmodium may carry out chemolithoautotrophic growth, and that Dp-green plasmodium may have used photolithoautotrophic growth in addition to chemolithoautotrophic growth. This may explain why the growth rate of Dp-green plasmodium was about three times higher than that of Dp-light brown plasmodium.

The formation of a green multinucleate plasmodium is especially important, in that it is presumably responsible for photosynthesis via chlorophyll. The amoeboid cells formed from the plasmodium seem to be self-assembled through the appropriate allocation of essential organelles from an apparently chaotic state in a time- and space-adjusted manner. According to the chlorophyll fluorescence observation, it is almost unlikely that free-living Dp-amoeboid cells derived from the green plasmodium can perform autotrophic growth by means of photosynthesis via chlorophyll, because most of them are devoid of green granules with chlorophyll fluorescence (see **Figure 8**). However, since a few number of amoeboid cells contain one or two chlorophyll fluorescence-positive granules like chloroplasts in the cytoplasm, it may be still possible that they will evolve into autotrophic cells which are able to undergo photosynthesis via chlorophyll in the process of long-term subculture.

The multinucleate plasmodium is behaviorally similar to that of a true slime mold such as *Physarum polycephalum,* except for the deficiency of chloroplasts [25]. When the multinucleate plasmodium of *Physarum polycephalum* is starved and light-irradiated, it moves to construction of fruiting bodies in which many spores are formed. Such a mode of spore formation seems somewhat similar to the creation of amoeboid cells from the autotrophic multinucleate plasmodia. In the case of autotrophic plasmodia, the red or green granular structures will probably function as organelles in coordination with the Dp-nucleus, as the morphological and behavioral characteristics of Dp-light brown and Dp-green plasmodia were stably retained during long-term successive cultures without a food source. Therefore, it is possible that the multinucleate plasmodium described above may be the most primitive structural form required for the initial conversion from heterotrophy to autotrophy. The optimum conditions for autotrophic cell growth are achieved when the growth rate of the host cell's nuclei is completely synchronized with those of the organelles, such as mitochondria and chloroplasts. Therefore, investigations into the optimal conditions necessary for autotrophic cell growth, as well as for the development of multinucleate plasmodia, will be required in future studies, as the growth rates of the Dp-light brown and Dp-green plasmodia are not sufficiently high at the present stage.

On electron microscopic observation, the central region of the Dp-green plasmodium was mainly composed of numerous *Synechocystis*-like bodies, in addition to disassembled *Rhodobacter* and Dp-derived mitochondria, as in the case of the middle and peripheral regions of multinucleate plasmodium. Because Dp-nuclei were not frequently observed in the multinucleate plasmodium, they may have been low in number or markedly damaged during the course of EM preparation. In Dp-green and Dp-light brown plasmodia, a large number of structurally modified mitochondria, each of which was surrounded by a layer of electron-dense membrane, were observed. A considerable number of studies have pursued the mechanisms behind the establishment of secondary endosymbiosis, mainly using unicellular red algae, such as *Cyanidioschyzon merolae* [26], green *Hydra* (*Hydra viridissima*) [27], green *Paramecium* (*Paramecium bursaria*) [28], photosynthetic sea slugs (*Elysia timida*) [29] etc.: *C. merolae* has the simplest eukaryotic cell system: a small haploid genome, one chloroplast, one mitochondrion, and other essential organelles in the fewest number of units necessary. In particular, numerous studies have been conducted on the genomic involvement and the precise mechanisms of cooperated organelle division [30, 31]. In green *Hydra* and green *Paramecium*, secondary endosymbiosis with eukaryotic *Chlorella* algae imparts various benefits to the host bodies through the supply of O_2 and organic compounds by photosynthesis in the *Chlorella* cells, which are mostly undigested in the *Hydra* and *Paramecium* bodies. Furthermore, the host bodies supply CO_2, NH_2, etc., to the captured *Chlorella* cells. In the case of *Elysia timida*, it steals from the algae *Acetabularia acetabulum* to gain the photosynthetic light reactions of the chloroplasts [29]. However, the relationship between the captured *Chlorella and Acetabularia* cells and the host cells appears to be temporal coexistence. In the present work, we have successfully illustrated an original mode of cyanobacterial endosymbiosis, previously considered unproven in the field of evolutionary biology. The main reasons for the successful creation of autotrophic cells seem to be the two-stage forced feeding of Dp-cells with photosynthetic bacteria, involving long-term culture with purple photosynthetic bacteria like *Rhodobacter,* and then feeding the green photosynthetic bacteria like *Synechocystis*, to promote endosymbiosis, as previously described. Incidentally, when Dp-amoebae, *Rhodobacter,* and *Synechocystis were* cultured separately on 2% inorganic agar, they hardly proliferated during at least 7 days of culture at 22˚C. Thus it is evident that the multinucleate plasmodia reported here are able to grow in an autotrophic manner, without taking in external nutrients such as bacteria. The utilization of *Synechocystis* as a food source was especially important because of its morphological nature: it is not too large (ca. 2 μm in diameter) and has a round shape; therefore, *Synechocystis* cells were relatively easily phagocytosed by the Dp-cells pre-cultured with *Rhodobacter*. Thus, we have finally succeeded in providing an experimental system to analyze the molecular and cellular mechanisms of autotrophic appearance in real-time using Dp-brown or Dp-green cell masses derived from heterotrophic soil wild-type Dp-amoebae.

The fact that the light-brown plasmodium can grow slowly but autotrophically even in complete darkness is a surprise to us. This might be due to chemolithoautotrophic growth. Unlike conventional heterotrophic microorganisms that consume carbohydrates and amino acids, Prokaryotic chemolithoautotrophs have evolved the capacity to utilize reduced chemical compounds to fix CO_2 and drive metabolic processes [32]. For instance, two species of *Rhodobacter* among the nonsulfur purple bacteria may exhibit aerobic chemolithoautotrophic growth with hydrogen as the electron donor [33].

Some unusual results were obtained regarding to the genetic background of Dp-green cell masses, as shown by the PCR analysis and genome wide analysis. That is, the results are not supporting data showing that the autotrophic organisms obtained are derived from host *D. purpureum* cells. In other words, however, these data seem to indicate that the genomic DNA of host Dp cells and mitochondrial DNA may be drastically modified by probably horizontal gene transfer (HGT) during the course of heterotrophic to autotrophic conversion to the extent that the prototype is cannot be discerned. On the other hand, the genome wide analysis of the green cell masses gave a somewhat unexpected result: some fragments were found that slightly resembled the gene sequence of free-living *Acanthamoeba*. Although it is currently unknown how this happened, it may be possible the host cells accidentally replaced Dp-cells with *Acanthamoeba* by contamination during the long-term culture process. Alternatively, it is also possible that genome fragments of *Acanthamoeba*, many bacteria and organelles were inserted into host Dp genome,

presumably through HGT. Mitotracker-Green is known to stain with specific proteins present in mitochondria [34]. Considering from the fact that this reagent is able to stain strongly mitochondria in amoeboid cells derived from the green plasmodium as well as in host Dp-amoeboid cells (see **Figure 6(C)** and **Figure S6**), it is evident that the stainability is well retained despite structural changes in mitochondria during conversion from heterotrophic to autotrophic growth. In this study, we succeeded in creating autotrophs from heterotrophic host cells by forcing two kinds of photosynthetic bacteria to ingest. The autotrophs obtained in this study, however, showed quite strange properties and behavior. Since great care has been taken in cell transplantation and subculture, it is unlikely that the unique autotrophs reported here are caused by the contamination of other organisms like living *Acanthamoeba*, but at this time, it cannot be completely ruled out that the host cell of the obtained autotrophs is not *Dictyostelium* but *Acanthamoeba*. In any case, the important points to be emphasized here is that the strange autotrophs obtained in the present work are different from any organism reported so far, and that they are created by changing nutrient sources. This will provide one useful experimental system in the field of synthetic biology.

DATA AND MATERIALS AVAILABILITY

All data needed to evaluate the findings are included in the paper and/or the Supplementary materials. Additional data related to this paper may be requested from the authors.

LIMITATIONS OF THE STUDY

The cell membrane structure in the created autotrophs is very fragile, thus resulting in failure of preservation of cell membrane systems during ordinary fixation and subsequent dehydration for electron microscopy. Therefore, we will need to find other methods, e.g. rapid freezing without chemical fixation in the future. In addition, in the nature of this study it will take another 5 - 6 years to carry out some reproduction experiments.

ACKNOWLEDGEMENTS

We thank E. Suzuki, H. Yamaoka, and Y. Miyanaga for useful discussions. We also thank K. Ohashi for his cooperation in chlorophyll autofluorescence observation.

AUTHOR CONTRIBUTIONS

Y. M designed the research, wrote the paper and did electron microscopic research. Y. M and T. A conducted the research and analyzed the data to establish a useful method for creating autotrophs from heterotrophs. T. A carried out the molecular genetic analysis to examine the approximate gene composition of the newly created organism. All authors read, discussed and approved the manuscript.

FUNDING

This research was supported partly by Japan Society for the Promotion of Science (JSPS) KAKENHI Grant Number JP19H00982.

CONFLICTS OF INTEREST

The authors declare that they have no competing interests.

REFERENCES

1. Braakman, R. and Smith, E. (2012) The Emergence and Early Evolution of Biological Carbon-Fixation. *PLOS Computational Biology*, **8**, e1002455. https://doi.org/10.1371/journal.pcbi.1002455
2. Gutekunst, C. (2018) Hypothesis on the Synchronic Evolution of Autotrophy and Heterotrophy. *Trends in Bi-*

ochemical Sciences, **43**,402-411. https://doi.org/10.1016/j.tibs.2018.03.008

3. Quayle, J.R. and Ferenci, T. (1978) Evolutional Aspects of Autotrophy. *Microbiological Reviews*, **42**, 261-273. https://doi.org/10.1128/mr.42.2.251-273.1978
4. Keeling, P.J. (2013) The Number, Speed, and Impact of Plastid Endosymbiosis in Eukaryotic Evolution. *Annual Review of Plant Biology*, **64**, 583-607. https://doi.org/10.1146/annurev-arplant-050312-120144
5. Keeling, P.J. (2004) Diversity and Evolutionary History of Plastids and Their Hosts. *American Journal of Botany*, **91**, 1481-1493. https://doi.org/10.3732/ajb.91.10.1481
6. Ohkawa, H., Hashimoto, N., Furukawa, S., Kadono, T. and Kawano, T. (2011) Forced Symbiosis between Synechocystis spp. PCC 6803 and Apo-Symbiotic *Paramecium bursaria* as an Experimental Model for Evolutionary Emergence of Primitive Photosynthetic Eukaryotes. *Plant Signaling & Behavior*, **6**, 773-776. https://doi.org/10.4161/psb.6.6.15239
7. Bonner, J.T. (1965) The Cellular Slime Molds. 2nd Edition, Princeton University Press, Princeton.
8. Maeda, Y. (2005) Regulation of Growth and Differentiation in Dictyostelium. *International Review of Cytology*, **244**, 287-332. https://doi.org/10.1016/S0074-7696(05)44007-3
9. Raper, K. (1984) The Dictyostelids. Princeton University Press, Princeton. https://doi.org/10.1515/9781400856565
10. Olive, L.S. (1975) The Mycetozoans. Academic Press, Cambridge.
11. Loomis, W.F. (1982) The Development of *Dictyostelium discoideum.* Academic Press, Cambridge.
12. Amagai, A., Takahashi, F., Usui, T., Abe, T. and Maeda, Y. (2014) Induction of Macrocyst Formation by ZYG1 in *Dictyostelium discoideum*. *Research Journal of Developmental Biology*, **1**, 1-7. https://doi.org/10.7243/2055-4796-1-2
13. Mackenzie, C., Eraso, J.M., Choudhary, M., *et al*. (2007) Postgenomic Adventures with *Rhodobacter sphaeroides*. *Annual Review of Microbiology*, **61**, 283-307. https://doi.org/10.1146/annurev.micro.61.080706.093402
14. Kaneko, T., Sato, S., Kotani, H., *et al*. (1996) Sequence Analysis of the Genome of the Unicellular Cyanobacterium Synechocystis sp. Strain PCC6803. II. Sequence Determination of the Entire Genome and Assignment of Potential Protein-Coding Regions (Supplement). *DNA Research*, **3**, 185-209. https://doi.org/10.1093/dnares/3.3.185
15. Lyons, T.W., Reinhard, C.T. and Planavsky, N.J. (2014) The Rise of Oxygen in Earth's Early Ocean and Atmosphere. *Nature*, **506**, 307-315. https://doi.org/10.1038/nature13068
16. Soo, R.M., Hemp, J., Parks, D., Fischer, W.W. and Hugenholtz, P. (2017) On the Origins of Oxygenic Photosynthesis and Aerobic Respiration in Cyanobacteria. *Science*, **355**, 1436-1440. https://doi.org/10.1126/science.aal3794
17. Hohmann-Marriott, M.F. and Blankenship, R.E. (2011) Evolution of Photosynthesis. *Annual Review of Plant Biology*, **62**, 515-548. https://doi.org/10.1146/annurev-arplant-042110-103811
18. Mulkidjanian, A.Y., Koonin, E.V., Makarova, K.S., *et al*. (2006) The Cyanobacterial Genome Core and the Origin of Photosynthesis. *Proceedings of the National Academy of Sciences of the United States of America*, **103**, 13126-13131. https://doi.org/10.1073/pnas.0605709103
19. López-García, P., Eme, L. and Moreira, D. (2017) Symbiosis in Eukaryotic Evolution. *Journal of Theoretical Biology*, **434**, 20-33. https://doi.org/10.1016/j.jtbi.2017.02.031
20. Schaap, P., Winckler, T., Nelson, M., *et al*. (2006) Molecular Phylogeny and Evolution of Morphology in the Social Amoebas. *Science*, **314**, 661-663. https://doi.org/10.1126/science.1130670
21. Chida, J., Araki, H. and Maeda, Y. (2014) Specific Growth Suppression of Human Cancer Cells by Targeted De-

livery of Dictyostelium Mitochondrial Ribosomal Protein S4. *Cancer Cell International*, **14**, Article No. 56. https://doi.org/10.1186/1475-2867-14-56

22. Maeda, Y. and Takeuchi, I. (1969) Cell Differentiation and Fine Structures in the Development of the Cellular Slime Molds. *Development, Growth & Differentiation*, **11**, 232-245. https://doi.org/10.1111/j.1440-169X.1969.00232.x
23. Gray, M.W. (1992) The Endosymbiont Hypothesis Revisited. *International Review of Cytology*, **141**, 233-357. https://doi.org/10.1016/S0074-7696(08)62068-9
24. Archibald, J.M. (2015) Endosymbiosis and Eukaryotic Evolution. *Current Biology*, **25**, R911-R921. https://doi.org/10.1016/j.cub.2015.07.055
25. Burland, T.G., Chainey, A.M., Dee, J. and Foxon, J.L. (1981) Analysis of Development and Growth in a Mutant of *Physarum polycephalum* with Defective Cytokinesis. *Developmental Biology*, **85**, 26-38. https://doi.org/10.1016/0012-1606(81)90233-5
26. Matsuzaki, M., Misumi, O., Shin, I.T., *et al.* (2004) Genome Sequence of the Ultrasmall Unicellular Red Alga *Cyanidioschyzon merolae* 10D. *Nature*, **428**, 653-657. https://doi.org/10.1038/nature02398
27. Habetha, M., Anton-Erxleben, F., Neumann, K. and Bosch, T.C. (2003) The Hydra Viridis/Chlorella Symbiosis. Growth and Sexual Differentiation in Polyps without Symbionts. *Zoology* (*Jena*), **106**, 101-108. https://doi.org/10.1078/0944-2006-00104
28. Blanc, G., Mozar, M., Agarkova, I.V., *et al.* (2014) Deep RNA Sequencing Reveals Hidden Features and Dynamics of Early Gene Transcription in *Paramecium bursaria* Chlorella Virus 1. *PLOS ONE*, **9**, e90989. https://doi.org/10.1371/journal.pone.0090989
29. Havurinne, V. and Tyystjärvi, E. (2020) Photosynthetic Sea Slugs Induce Protective Changes to the Light Reactions of the Chloroplasts They Steal from Algae. *Elife*, **9**, e57389. https://doi.org/10.7554/eLife.57389
30. Fujiwara, T., Tanaka, K., Kuroiwa, T. and Hirano, T. (2013) Spatiotemporal Dynamics of Condensins I and II: Evolutionary Insights from the Primitive Red Alga *Cyanidioschyzon merolae*. *Molecular Biology of the Cell*, **24**, 2515-2527. https://doi.org/10.1091/mbc.e13-04-0208
31. Yoshida, Y., Kuroiwa, H., Misumi, O., *et al.* (2010) Chloroplasts Divide by Contraction of a Bundle of Nanofilaments Consisting of Polyglucan. *Science*, **329**, 949-953. https://doi.org/10.1126/science.1190791
32. Nybo, S.E., Khan, N.E., Woolston, B.M. and Curtis, W.R. (2015) Metabolic Engineering in Chemolithoautotrophic Hosts for the Production of Fuels and Chemicals. *Metabolic Engineering*, **30**, 105-120. https://doi.org/10.1016/j.ymben.2015.04.008
33. Paoli, G.C. and Tabita, F.R. (1998) Aerobic Chemolithoautotrophic Growth and RubisCO Function in *Rhodobacter capsulatus* and a Spontaneous Gain of Function Mutant of *Rhodobacter sphaeroides*. *Archives of Microbiology*, **170**, 8-17. https://doi.org/10.1007/s002030050609
34. Kusano, S. and Hayashida, O. (2016) Development of Tetraphenylethylene-Appended Tetraazacyclophanes: The Evaluation of Aggregation Induced Emission Property and the Application for Biomolecular Sensing. *Chemistry Letters*, **45**, 1084-1086. https://doi.org/10.1246/cl.160528

SUPPLEMENTARY MATERIALS

Supplementary figures for this article are available at the back of this manuscript.

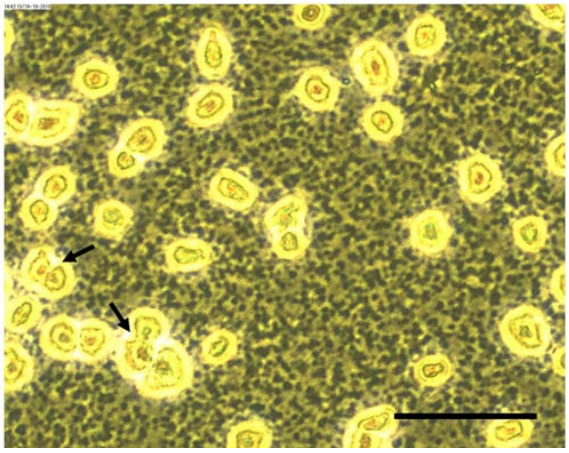

Figure S1. Free-living amoeboidcells and a green multinucleate plasmodium formed outside a Dp-green cell mass. Note that some cells (arrows) are dividing and, and each amoeboid cell contains both red and green pigments. In the GMN, numerous dark-blue granules, most of which are probably *Synechotiscis*-derived structures, are observed. Bar, 80 μm.

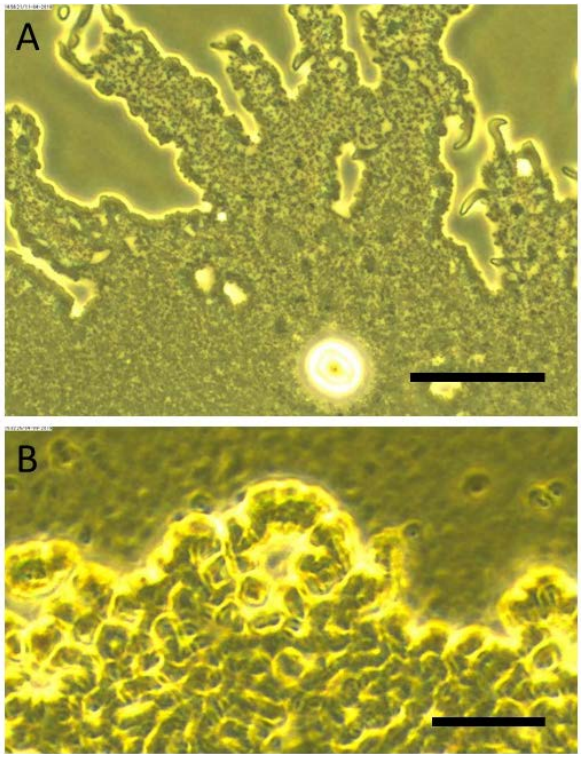

Figure S2. The outermost regions of a multinucleate green plasmodium. (A) In the thin plasmodium, many granular structures. (B) Cells that continue to be made at the outermost region of the plasmodium probably by the self-organization of the multinucleate body are visible. Bar, 80 μm.

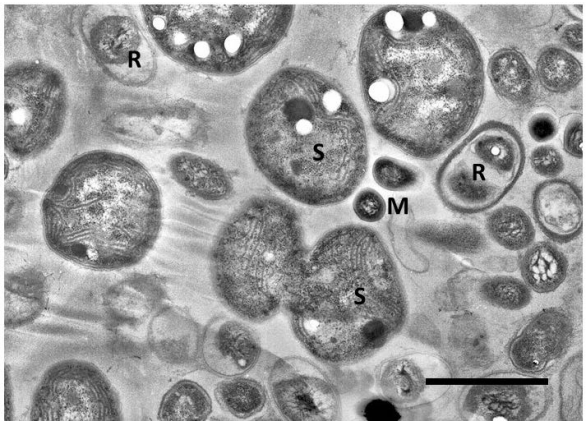

Figure S3. The fine structure of a multinucleateplasmodium near the central region of a Dp-green cell mass. In this region, *Synechocystis*-derived bodies (S) are predominantly present, and other structures such as *Rhodobacter*-derived bodies (R) and Dp-derived mitochondria (M) are also visible. Bar, 1 μm.

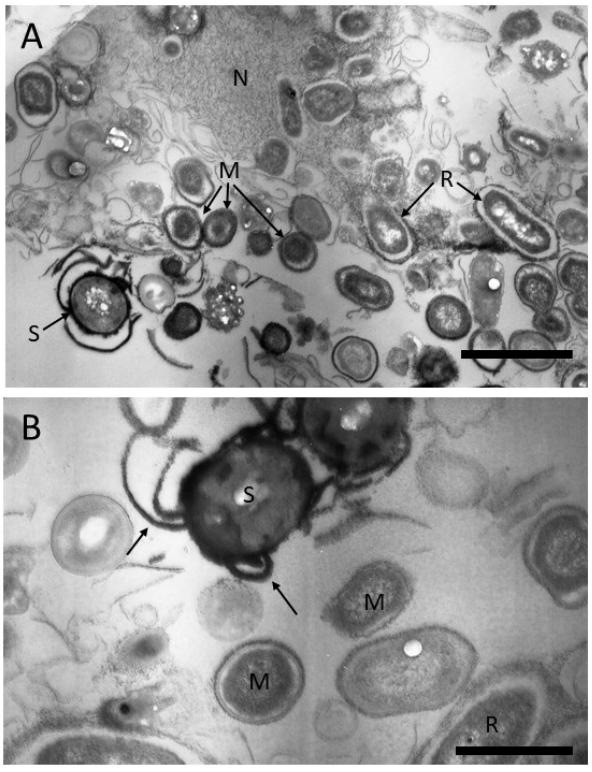

Figure S4. Ultrastructure of an amoeboid cell derived from the green plasmodium. (A) In the cytoplasm, there were numerous structures including unique mitochondria (M), *Synechocystis*-derived structures (S), and *Rhodobacter*-derived structures (R), all of which were surrounded by electron-densemembranes. The feature marked with the symbol N is possibly a Dp-derived nuclear region, judging by its morphology. Bar, 2 μm. (B) High magnification image of the Dp-green cell. Note that the highly electron-dense membranes (arrows) are well developed on the surface of the *Synechocystis*-derived structure (S). M, unique mitochondria: R, *Rhodobacter*-derived structure. Bar, 1 μm.

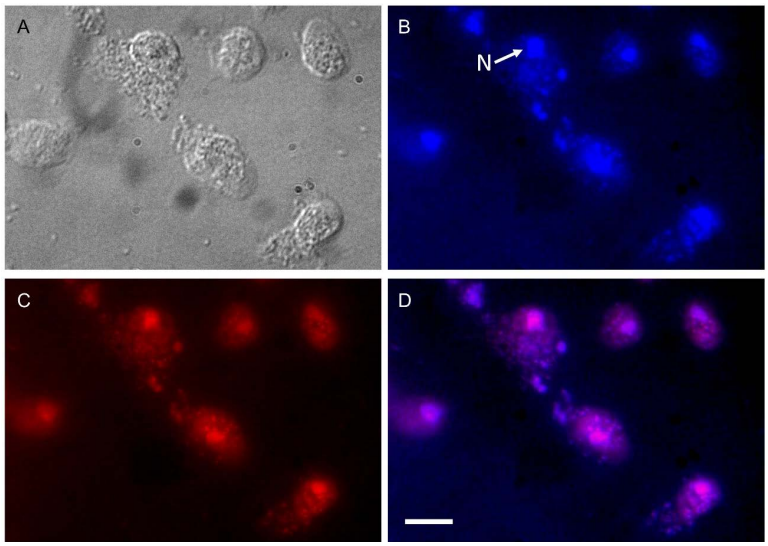

Figure S5. Staining of host *D. purpureum* (Dp) amoeboid cells with DAPI and MitoTracker-Green. (A) DIC (differential interference contrast) microscopic image. Several amoeboid cells at the vegetative growth phase are visible. (B) DAPI-staining image of the same region with (A). In addition to cell nuclei (N), a considerable number of mitochondria are stained. (C) MitoTracker-Green-stained cells of the same region as (A). (D) The merged image of DAPI-staining (B) and MitoTracker-Green-staining (C). The original green-colored granular stains with MitoTracker-Green were artificially converted to red in (C) in order to merge with the DAPI-staining in (B). Note pink granules with mitochondrial DNA and certain mitochondrial proteins. Some of the pink granules seem to be in close to the nucleus. Blue granules are probably undigested *Klebsiella aerogenes* present in phagosomes. Bar, 10 μm.

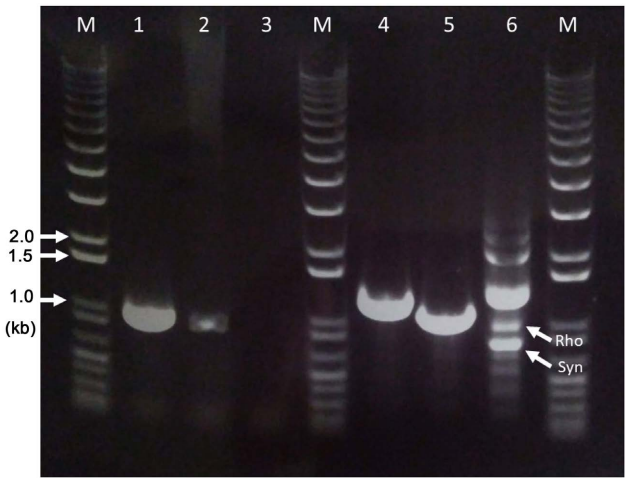

Figure S6. Genomic PCR of Dp-green cell masses and host *Dictyostelium* cells. Agarose gels loaded with amplicons from genomic PCR as described in Materials and Methods. PCRs were performed with Dd-MRP4 primers (Lane 1 to 3) and 5.8S rRNA primers (Lane 4 to 6). Genomic templates used were isolated from *D. discoideum* (Lane 1 and4), *D. purpureum* (Lane 2 and 5) and Dp-green cell masses (Lane 3 and 6). Lanes marked M are size markers. Arrows marked Rho and Syn indicate amplicons identified as partial sequences of *Rhodobacter* and *Synechocystis*, respectively.